Organelle DNA degradation contributes to the efficient use of phosphate in seed plants

Tsuneaki Takami[1], Norikazu Ohnishi[1], Yuko Kurita[2,4], Shoko Iwamura[2], Miwa Ohnishi[2], Makoto Kusaba[3], Tetsuro Mimura[2] & Wataru Sakamoto[1]*

[1] Institute of Plant Science and Resources, Okayama University, Kurashiki, Japan

[2] Department of Biology, Graduate School of Science, Kobe University, Kobe, Japan

[3] Graduate School of Science, Hiroshima University, Higashi-Hiroshima, Japan

[4] Present address: Faculty of Agriculture, Ryukoku University, Otsu, Japan

* e-mail: saka@okayama-u.ac.jp

Corresponding author: Wataru Sakamoto

Mailing address: Institute of Plant Science and Resources
Okayama University
2-20-1 Chuo, Kurashiki, Okayama 710-0046
Japan

Telephone and Fax: +81-86-434-1206

Email: saka@okayama-u.ac.jp

One Sentence Summary: DNA retained in the endosymbiotic organelles – chloroplasts and mitochondria – of seed plants influences growth in phosphate-limited conditions through a degradation mechanism implemented by DPD1 exonuclease.

Mitochondria and chloroplasts (plastids) both harbor extra-nuclear DNA that originates from the ancestral endosymbiotic bacteria. These organelle DNAs (orgDNAs) encode limited genetic information but are highly abundant, with multiple copies in vegetative tissues such as mature leaves. Abundant orgDNA constitutes a significant pool of organic phosphate along with RNA in chloroplasts, which could potentially contribute to phosphate recycling when it is degraded and relocated. However, whether orgDNA is degraded nucleolytically in leaves remains unclear. In this study, we revealed the prevailing mechanism, in which organelle exonuclease DPD1 degrades abundant orgDNA during leaf senescence. The DPD1 degradation system is conserved in seed plants, and more remarkably we found that it was correlated with the efficient use of phosphate when plants were exposed to nutrient-deficient conditions. The loss of DPD1 compromised both the relocation of phosphorus to upper tissues and the response to phosphate starvation, resulting in reduced plant fitness. Our findings highlighted that DNA is also an internal phosphate-rich reservoir retained in organelles since their endosymbiotic origin.

Mitochondria and chloroplasts (plastids) originate respectively from the endosymbiosis of ancestral α-proteobacterium and cyanobacterium, ca. 1.5 billion years ago [1]. Reflecting this endosymbiotic origin is the retention of their own DNA genomes and transcription/translation machineries. During the evolution of eukaryotic cells, however, most genes from these endosymbionts have been transferred to the nucleus, and only a small proportion of the ancestral genes remain within each organelle [2-4]. In the model plant *Arabidopsis thaliana*, for example, only 87 proteins are synthesized in chloroplasts, whereas all other constituent proteins are encoded in the nuclear genome [5]. Present eukaryotes, therefore, require the coordinated regulation between mitochondria/chloroplasts and the nucleus to fulfill organelle functionality [6-9].

In contrast to their limited genetic capacity, organelle genomes of relatively small size are known to be highly abundant, with multiple copies in each organelle. A striking example is leaf mesophyll cells, in which chloroplast DNA (cpDNA) accounts for ca. 30% of cellular total DNA, with an estimated >1,000 copies per cell [10-13]. Typically, an *A. thaliana* mesophyll contains ~80 chloroplasts, resulting in >10 copies per chloroplast on average. Plastid DNA (ptDNA) copy numbers appear to vary in different species and in different plastid types, and they reach up to ~10,000 in developing leaves. As a consequence of the abundant DNA and protein synthesis, plastids contain a substantial amount of nucleic acids, which constitute a major pool of total cellular phosphorus (P) in leaves [14,15]. Reportedly, chloroplast ribosomal RNAs account for the largest organic P pool, making up approximately half of the total nucleic acids pool [15]. The multiple copies of ptDNA represent a considerable P pool. Excess ptDNA can be dispensable without affecting organelle functionality or cell viability, potentially providing a source of organic P for relocation when degraded. However, whether the amount of cpDNA/ptDNA is controlled by degradation in mature leaves has long been unclear [16,17]. Little is known about the enzymatic degradation mechanism and its possible impact on the efficient use of the internal P pool in endosymbiotic organelles.

In reproductive organs, several nucleases targeted to the endosymbiotic organelles have been reported to digest DNA [18,19]. In animals, mitochondrial EndoG nuclease expressed during male gametogenesis has been reported, which secures maternal inheritance of mtDNA [20]. In a green alga, uniparental disappearance of orgDNA during mating occurs, although the nuclease responsible remains unclear [21]. In flowering plants, we reported that DPD1 exonuclease degrades orgDNA in male gametophytes [22]. However, DNA degradation by DPD1 *per se* does not contribute to maternal inheritance. Therefore, we postulate that DPD1 has functions other than the control of maternal inheritance. In this study, we demonstrated that in addition to its role in pollen, DPD1 degrades orgDNA in leaves undergoing senescence

where nutrients are recycled through various macromolecule degradation mechanisms. DPD1 presents a determinate mechanism of orgDNA degradation conserved in plants. Moreover, this orgDNA degradation was shown to affect the efficient use of phosphate (Pi) positively when exposed to starvation conditions. We discuss a novel aspect of orgDNA, likely sensing Pi availability and acting as an internal reservoir of Pi, through degradation mediated by DPD1 in seed plants.

Results

Exonuclease activity of DPD1 confined to DNA but not RNA. We have shown that DPD1 is conserved in angiosperms but it was not detected in mosses or green algae, suggesting that it emerged during the evolution of flowering plants [22]. Our search in the PLAZA database allowed us to isolate 43 DPD1 homologues from 35 plant species (Supplementary Fig. 1). Consistently, no DPD1 homologues were present in microorganisms or bryophytes, although its presence extended to gymnosperms (coniferous plants such as *Pinus*, *Picea*, *Pseudotsuga* and *Gnetum*) (Supplementary Fig. 1), supporting this specific emergence of DPD1 in seed plants (spermatophytes).

DPD1, which exhibits exonuclease activity and is targeted to both mitochondria and plastids, is unique in that most of the cell death-associated nucleases identified previously in plants are S1-type or Staphylococcal endonucleases [23]. Because these endonucleases digest both RNA and DNA when single-stranded, we first tested if DPD1 has substrate specificity. Our in vitro nuclease assay, conducted using a purified DPD1 C-terminally fused to histidine tag and synthesized oligonucleotides as substrates (Fig. 1a), demonstrated that DPD1 degraded only DNA and not RNA, irrespective of whether it was single-stranded or double-stranded (Fig. 1b). This activity depended on Mg^{2+} (Fig. 1c) and was inhibited when a substrate 3'-end-labeled with a fluorescent dye (6-FAM) was used (Fig. 1b–d). We inferred that DPD1 is a 3' to 5' Mg^{2+}-dependent deoxyribo-exonuclease, whose activity can be detected in physiological conditions equivalent to chloroplast stroma (Mg^{2+} concentration of >0.02 mM, temperature 22°C and pH 7.0–8. 0, Supplementary Fig. 2) [24]. Given its heterogeneous forms, DPD1 alone can degrade at least a portion of orgDNAs processively, if they have a free 3' end.

CpDNA degradation during leaf senescence. Our earlier survey of *Arabidopsis* transcriptome data predicted that *DPD1* transcripts accumulate in senescing leaves as well as in pollen [23]. To examine if DPD1 plays a role in vegetative tissues, detached *Arabidopsis* leaves were subjected to dark-induced senescence (see *Methods*), and orgDNA degradation

was monitored by quantitative PCR (qPCR). CpDNA levels in wild-type (ecotype Columbia [Col]) leaves declined apparently as senescence proceeded during incubation in the dark (Fig. 2a). When normalized using haploid nuclear DNA levels, we estimated the cpDNA copy number before the onset of senescence as approximately 400–600, which was similar to that reported previously (Fig. 2b) [13]. After 5 days in darkness, DNA levels declined substantially to less than 100 copies. Concomitant with cpDNA decline, our quantitative RT-PCR (qRT-PCR) analysis showed that *DPD1* is upregulated (Fig. 2c), similarly or slightly earlier than senescence-related genes (Supplementary Fig. 3). Importantly, cpDNA levels did not decline in a *dpd1* mutant and tended to stay constant (Fig. 2b). Retention of cpDNA in *dpd1* was verified using digital PCR (Supplementary Fig. 4) and cytological observations of senescing leaves (Fig. 2d). Taken together, we concluded that DPD1 degrades cpDNA during leaf senescence.

Although the mechanism for maintaining ptDNA quantity remains unclear, a defect in DNA replication has been shown to affect ptDNA copy number adversely [25]. DNA polymerase in plant organelles is a bacterial-type pol I [26]. In *Arabidopsis*, two isoforms have been reported, pol I-a and pol I-b, of which pol I-a plays the major role in ptDNA replication. Introduction of *pol I-a2* into *dpd1* appeared to decrease the copy number of cpDNA, whereas cpDNA stayed high during senescence (Fig. 2e). Therefore, our results revealed an epistatic effect of DPD1-mediated cpDNA degradation over DNA synthesis.

MtDNA degradation during leaf senescence. We next examined whether mitochondrial DNA (mtDNA) levels also declined in senescing leaves. The results showed a similar trend to cpDNA; mtDNA levels declined in Col as senescence proceeded, although they tended to stay constant in *dpd1*. Therefore, we concluded that DPD1 also degrades mtDNA during leaf senescence. However, the estimated copy number was found to be very low, ranging from around a few copies per nuclear DNA even before dark incubation (Supplementary Fig. 5a). To address whether mtDNA levels decreased during leaf maturation, we examined 2-week-old seedlings grown in Murashige and Skoog (MS) plates to estimate mtDNA copy number. The result showed that approximately 20 copies of mtDNA were detected in young seedlings (Supplementary Fig. 5b). We observed a slight increase of the mtDNA copy number (approximately 25) in *dpd1* compared with Col, consistent with previous reports. These results indicated that the mtDNA copy number declines before leaf maturation, which is independent of DPD1. Although the mechanism responsible for this mtDNA degradation remains unclear, the estimated copy number of mtDNA was consistent with previous reports describing that only a limited amount of mtDNA is detectable in mature leaves [27,28]. In contrast to this

shortage in mtDNA, plant mitochondria are known to undergo active fusion and fission [8,29]. This dynamic behavior of mitochondria might account for the proposed sharing of genomic information between each mitochondrion. We concluded that orgDNA degradation proceeds in both organelles, but the majority occurs in chloroplasts.

A weak stay-green phenotype in *dpd1*. A careful examination of senescing leaves revealed that *dpd1* displayed more greenness than Col and a *dpd1* line complemented by *DPD1* (G31) (Fig. 3a–b, Supplementary Fig. 6). This stay-green phenotype defines DPD1 as a factor accelerating senescence and cell death. Conversely, prolonged chloroplast functionality might be detectable in the *dpd1* mutant. To address this, we first assessed the expression levels of chloroplast genes. qRT-PCR analysis revealed that the senescence-dependent decline in chloroplast-encoded transcripts was retarded in *dpd1* (Fig. 3c and Supplementary Fig. 7). We inferred that the more abundant transcripts in *dpd1* partly explained the stay-green phenotype, and that cpDNA degradation with DPD1 resulted in a concomitant reduction in the chloroplast RNA pool. Subsequently, we tested if the stay-green phenotype in *dpd1* prolonged chloroplast functionality. Photosynthetic activity, as measured by the carbon dioxide assimilation rate in the same attached leaves grown for 2 weeks, appeared to be maintained for longer in *dpd1* than Col (Fig. 3d, e). Together, these results confirmed that DPD1 accelerates senescence, although senescence still proceeds without DPD1.

Growth defect of *dpd1* in Pi starvation conditions. The synergistic action of DPD1 on leaf senescence led us to postulate that cpDNA degradation is associated with nutrient availability. As a tradeoff between leaf longevity and nutrient deficiency, *dpd1* prolongs photosynthesis, but it might impair growth in conditions with limited inorganic compounds. To test this possibility, we established hydroponic culture to grow Col and *dpd1* (Supplementary Fig. 8) and observe the subsequent response to nitrogen or Pi deprivation (-N or -P, respectively) was investigated [30]. First, based on our standard hydroponic conditions (1/4 MS medium), we found that Col grew better than *dpd1* as estimated from the weight of aerial parts (Fig. 4a). This result was unexpected because no apparent difference was observed previously when they were grown in soil. Supplementing the hydroponic media with additional Pi rescued the defective growth of *dpd1* (Fig. 4a), suggesting that *dpd1* is specifically compromised in P availability. Additional Pi did not have significant effect in Col.

We next examined how Col and *dpd1* respond to -N and -P in our standard hydroponic culture (see *Methods*). In principle, both starvation conditions attenuated plant growth by reducing the weight of aerial parts (Supplementary Fig. 9a, b). However, *dpd1* appeared to

differ from Col in responding to -P. In -N conditions, both lines showed a pale color with slight anthocyanin accumulation, but no phenotypic difference was detectable. By contrast, -P conditions produced a profound growth defect in *dpd1*, which was characterized by reduced growth and substantial accumulation of anthocyanin (Fig. 4b) [31]. Such typical symptoms of -P conditions were not observed in Col. These results suggested that the efficient use of exogenous Pi was compromised in *dpd1* by the lack of orgDNA degradation. When exposed to -N or -P conditions, qPCR demonstrated that cpDNA levels in Col leaves underwent degradation upon -N or -P similarly to dark-induced senescence, whereas degradation was inhibited in *dpd1* (Fig. 4c, d).

Low fitness and P relocation of *dpd1* in Pi starvation conditions. To ascertain the compromised response to -P, we measured seed production in Col and *dpd1.* First, seed numbers in plants grown in soli or hydroponic culture were counted. The hydroponic culture reduced seed production rate in Col, even in control conditions (1/4 MS), to approximately 80% of that grown in soil (Fig. 4e and Supplementary Fig. 9b). We also observed that the seed production rate was lower in *dpd1* than Col. Remarkably, -P reduced seed production, even in Col, to approximately 50% of that in the control conditions, whereas *dpd1* consistently showed a greater reduction in seed set than Col. Although our data indicated that *dpd1* exhibited lower fitness in -P conditions than Col, it was possible that this resulted from the delayed senescence in *dpd1*, as evidenced by its weak stay-green phenotype. To compare this effect, we also measured seed set in -N conditions. The results showed no significant difference in seed set between Col and *dpd1* (Fig. 4e). Therefore, nutrient starvation *per se* did not alter the sink capacity, instead *dpd1* had a lowered fitness confined to -P conditions.

To examine whether the reduced fitness in *dpd1* resulted from altered P remobilization, we measured the P content in leaves of Col and *dpd1* in -P conditions. Assuming that degradation products of orgDNA contribute to seed set by relocating the catabolic products to reproductive organs, we expected to have lower P levels in the lower leaves of Col than in *dpd1*. ICP-MS measurement of the total P concentration indeed showed that Col leaves at 2 weeks after Pi deprivation relocated a significant greater amount of P from the lower leaves (leaves preexisting before P deprivation) to upper leaves (leaves that emerged after the start of -P treatment) (Fig. 4f). By contrast, no significant P relocation was detected in *dpd1*. The adverse effect of P redistribution between Col and *dpd1* in -P conditions was, as expected, shown to correlate with our fitness results. We concluded that orgDNA degradation contributes to efficient P relocation, particularly when plants face P-limited conditions.

Global response to nutrient starvation in *dpd1*. We next investigated global changes in the transcriptome in -P conditions using RNA seq (Fig. 5, Supplementary Fig. 10 and Supplementary Fig. 11). RNA was isolated from Col and *dpd1* leaves either subjected to continuous growth in 1/4 MS or to Pi deprivation (*n*=3, dataset is presented as Supplementary Table 1 and Supplementary Table 2). Comparison of the gene expression profiles revealed that the response to -P starvation was profoundly altered between Col and *dpd1* (Fig. 5a). The number of genes that were differentially expressed upon -P treatment was 766 in Col, of which 655 genes were upregulated. In contrast, only 114 were differentially expressed in *dpd1*; 96 genes were upregulated (Supplementary Fig. 10a). Col and *dpd1* shared 99 genes, among which 86 upregulated genes had GO terms related to phosphate starvation, photosynthesis, flavonoid biosynthesis and dephosphorylation.

To investigate these genes further, we specifically examined a set of genes that were categorized as related to Pi starvation response (PSR), mainly connected by a limited supply of inorganic Pi in the root environment (Supplementary Table 3) [33]. Of 193 genes specified as being involved in the PSR, we were able to extract 192 genes; among these, 123 and 40 genes were shown to be upregulated in Col and *dpd1*, respectively, at the significance level of false discovery rate [FDR] <0.05 (Fig. 5c). We also specifically examined the gene set that was reported as being under the control of the PHR1 transcription factor (PHR regulon, Supplementary Table 4) [33]. Of 161 genes, 74 and 39 genes were upregulated in Col and *dpd1*, respectively (Supplementary Fig. 10b). Based on these results, we inferred that the global gene expression in response to -P conditions was compromised in *dpd1*. It was conceivable that orgDNA degradation and PSR are mutually interconnected, and that proper PSR requires orgDNA degradation.

We scrutinized the PSR genes differentially expressed between Col and *dpd1* (Supplementary Table 3 and Supplementary Fig. 10c). Upregulated genes in Col included those encoding Pi transporter (PHT1;9, PHT5, PHT3;2, PHT2, PHT1;4), purple acid phosphatase (PAP23, PAP7, PAP2, PAP22, PAP25, PAP17, PAP24, PAP14, PAP12), enzymes for lipid biosynthesis (MGD2, DGD2, MGDC, SQD1, SQD2) and RNase (RNS1), with which phosphate uptake or utilization is shown to be maximized in -P conditions. It was noteworthy that in *dpd1*, upregulation of the Pi transporter genes is limited to PHT1;9 and PHT5, although most of the purple acid phosphatase genes (*PAP22*, *PSP25*, *PAP2*, *PAP23*, *PAP12*, *PAP17*, *PAP24*) are also upregulated. In contrast to the genes preferentially upregulated in Col, we found several genes with expression levels that were higher in *dpd1* than Col (PPCK2, FHL and PLDZETA2). Overall, our RNA seq analysis revealed that the response to -P conditions was disturbed severely by the loss of orgDNA degradation.

Suppression of transporter genes in *dpd1*, but not the *PAP* gene, implied that the impact of orgDNA degradation in PSR is complex and is correlated with intra-cellular and inter-cellular Pi relocation.

To assess whether the altered transcriptome in *dpd1* was rather specific to PSR, we also performed RNA seq with the plants exposed to -N conditions (*n*=3, dataset is presented as Supplementary Table 5 and Supplementary Table 6). Both Col and *dpd1* presented many genes that were differentially regulated (1,768 for Col and 961 for *dpd1,* Supplementary Fig. 11a), suggesting that -N conditions generally impacted a broad range of genes (Fig. 5b). To investigate the -N response specifically, we focused on two sets of genes that have been reported previously to respond to -N conditions (Fig. 5d, Supplementary Fig. 11b, Supplementary Table 7, and Supplementary Table 8) [32,34]. Comparison of these transcriptomes indicated that both Col and *dpd1* displayed similar expression profiles based on the values at the median and upper/lower quartile, although *dpd1* had a slightly reduced number of the genes than Col (Fig. 5d). These results were consistent with the growth defect and fitness observed in -N conditions (Supplementary Fig. 9a). Taken together, we concluded that *dpd1* was compromised in PSR and that orgDNA degradation acts in the efficient use of Pi.

OrgDNA degradation mediated by DPD1 in natural conditions. To verify the role of orgDNA degradation, we questioned if it occurs in the natural environment. Seasonal remobilization of nutrients such as N and P from senescing leaves has been documented as being important in deciduous trees [35]. In *Populus alba*, we have shown previously that about 60% of P in leaves was remobilized before the autumn leaf fall [36,37]. CpDNA degradation has also been reported in a tree [38]. Therefore, we considered that *P. alba* is suitable to test if DPD1-mediated orgDNA degradation coincides with P remobilization. We conducted leaf sampling from a field-grown *P. alba* tree (Supplementary Fig. 12), every month from the stage of bud break (April) up to complete leaf fall (November) (Fig. 6a). Estimation of cpDNA copy number by qPCR revealed that, in general, cpDNA was more abundant in spring and decreased gradually in autumn (Fig. 6b). Similarly to the case in *Arabidopsis*, mtDNA levels were much lower throughout the season (Fig. 6c). A small spike in orgDNA levels detected in the summer was likely due to leaf regeneration, which was consistent with P measurements in our previous study [36]. Cytological observation of cpDNA was consistent with qPCR, showing holistic disappearance of cpDNA in autumn leaf samples (Fig. 6d).

qRT-PCR analysis of these samples, designed based on the available reference sequence from *P. trichocarpa*, demonstrated that a poplar *DPD1* homologue was highly

upregulated toward leaf fall, with the highest level observed in November (Fig. 6e). We obtained these data from two consecutive seasons (2015 and 2016), which all showed upregulation of *DPD1* that accompanied concomitant upregulation of senescence-related genes (Supplementary Fig. 14). We also confirmed *DPD1* upregulation in laboratory conditions, which mimicked natural seasonal changes and leaf fall with three defined growing conditions (Fig. 6f) [36]; *DPD1* was specifically upregulated at Stage 3, corresponding to autumn/winter (Fig. 6g and Supplementary Fig. 15). Therefore, all of these experiments confirmed the contribution of the *DPD1* system during natural leaf fall, during which Pi is redistributed.

Discussion

CpDNA degradation in leaf tissues has been documented for more than two decades [39,40]. However, whether DNA is degraded nucleolytically has been controversial, partly because of technical limitations of qPCR, variation within species and tissues, and a lack of mechanistic insights [16,17,41]. Our studies with DPD1 uncovered the prevailing degradation mechanism among seed plants. We focused initially on male gametophytes (pollen), because the disappearance of orgDNA in male germ cells is often related to maternal inheritance [42-44], as evidenced in animal EndoG [18,20]. Although we identified DPD1 exonuclease through forward-genetic mutant screening [22,45], orgDNA was shown to be degraded mainly in pollen vegetative cells, which deliver sperm cells to ovules but do not contribute to fertilization. In fact, we did not observe a contribution of DPD1 to the maternal inheritance mode of mtDNA [22], which led us to reconsider the physiological role of orgDNA degradation mediated by DPD1. Here, we demonstrated that both in an annual plant (*Arabidopsis*) and a deciduous tree (*P. alba*), the DPD1 system operates on orgDNA degradation in vegetative tissues, toward the final stage of leaf lifespan for Pi availability. These results revealed that the primary role of the DPD1 system is associated with the efficient use of Pi, rather than orgDNA inheritance.

During leaf senescence, relocating internal macronutrients to the upper and reproductive tissues plays a critical role in maximum fitness [46,47]. Catabolism of macromolecules stored in chloroplasts is well described, including Rubisco, photosynthetic antenna protein, lipids and pigments, which act mainly in relocating N [48,49]. Our finding adds orgDNA to the macromolecules undergoing degradation [23,41]. It is noteworthy that a substantial portion of orgDNA resides in chloroplasts of fully expanded leaves, whereas only a limited number of mtDNAs exist [10,13,28]. Although DPD1 is dual targeted to both organelles, its dominant role seems to be in chloroplasts/plastids. Conceivably, orgDNA degradation is beneficial in pollen vegetative cells because male gametophytes, once formed, are isolated

from other part of tissues, which hampers their ability to receive external P efficiently. Conservation of the DPD1 system even in evergreen coniferous species (Supplementary Fig. 1) implicates that DPD1 has emerged during the evolution of microsporophytes, rather than the evolution of leaf senescence.

Several lines of evidence were presented to demonstrate the correlation of orgDNA with Pi starvation. First, *dpd1* showed defective growth in our standard hydroponic culture, which was then rescued by supplementing with additional Pi (Fig. 4a). Second, *dpd1* showed reduced fitness as well as typical symptoms in -P conditions (Fig. 4e). Third, these deficiencies in *dpd1* were not detected in -N conditions but rather specific to -P conditions. Finally, RNA seq analysis in -P conditions indicated that *dpd1* had compromised accumulation of PSR genes (Fig. 5). All these results suggested that orgDNA degradation participates in the efficient use of Pi. The most likely model to explain these results is that orgDNA itself acts as a P pool and is subjected to degradation for the redistribution of Pi (Supplementary Fig. 15, model 1). Consistent with this, upregulation of DPD1 during autumn leaf fall in *P. alba* coincided with the relocation of P from leaves (Fig. 6), which accounts for 60% of total P [36]. Although whether orgDNA serves as a significant pool of internal P awaits further investigation, we inferred that the lower fitness in *dpd1* could be explained by this reservoir model. The alternative model is that some orgDNA degradation product(s), such as nucleotides or their catabolic components, act as a positive sensor of PSR (Supplementary Fig. 15, model 2). Lack of these products may prevent plants in -P conditions from responding to P deficiency properly, which leads to lower fitness. Although we cannot exclude these two possibilities mutually, our data revealed an interconnection between orgDNA degradation and the efficient Pi use.

In leaves, nucleic acids constitute the most abundant Pi esters along with phospholipids [15,50]. Breakdown of nucleic acids and/or enzymes for the biosynthesis of galacto- and sulpho-lipids to remodel phospholipids are induced as a part of PSR, along with purple acid phosphatases that hydrolyze Pi monoesters [51,52]. We confirmed these PSR in our RNA seq data [33]. Based on the results presented in this study, we considered that DNA degradation in endosymbiotic organelles also contributes to PSR. The nucleic acid P pool, representing 40–60% of the total internal organic P, consists of RNA and DNA, with ribosomal RNA as the largest pool [15,50]. To degrade these large P pools, endonucleases are upregulated. RNS1 and RNS2 are the major ribonuclease that supposedly degrade cytosolic or extracellular RNAs [53]. BFN1 has been reported to be upregulated during leaf senescence and to degrade single-stranded DNA/RNA [54,55]. These findings imply RNA as a major P pool for relocation, whereas DNA has been considered as a minor P pool because of its indispensability. By

contrast, DPD1 is unique in that it is confined to plastids and mitochondria and degrades 'dispensable' orgDNA. Given that total DNA represents 20–30% of total nucleic acids in leaves [7,56], we estimated that orgDNA comprises 6–9% of total nucleic acid pool. Although minor, the dispensable orgDNA pool may serve as a safe guard of the Pi reservoir, consequently giving an advantage in -P conditions. In principle, extra internal Pi is considered to be stored in vacuoles [57,58]. While transporting free Pi out of vacuoles plays a critical role in -P management [59], the contribution of chloroplasts remained elusive. During leaf senescence, dismantling of chloroplast compounds through enzymatic degradation and/or autophagic processes are recognized to be crucial [48,60]. Our finding reinforces the importance of chloroplasts for relocating macronutrients, particularly for P.

Lack of orgDNA degradation in *dpd1* caused a weak stay-green phenotype, but leaf senescence proceeded almost normally. Therefore, we considered that orgDNA degradation is not a decisive factor controlling the onset of leaf senescence. As a consequence of more cpDNA being retained (Fig. 3c), chloroplasts showed prolonged functionality because of the retarded decline in chloroplast transcripts. We inferred that orgDNA indirectly determines leaf lifespan, by balancing a tradeoff between prolonged photosynthesis and nutrient demand (Supplementary Fig. 15). In general, leaf senescence is associated with nutrient starvation, and an overlap between PSR and senescence-induced genes has been reported [50]. Given the fact that orgDNA declines in response to both -N and -P but PSR is predominantly compromised in *dpd1* (Fig. 5), we considered that the primary role of orgDNA degradation is likely to be to maximize P availability in leaves. One possibility of orgDNA contributing to leaf senescence could be a 'point of no return', which is proposed to define the stage that the senescence process cannot be reversed [47]. It is known that senescence is reversible up to a certain point by providing additional nutrients. Conceivably, senescence is no longer reversible when cpDNA is completely lost.

DPD1 is homologous to DnaQ, an epsilon proofreading subunit of *E. coli* DNA polymerase III [22,41]. Given that orgDNA replication adopts Pol I [26], it remains unclear how DPD1 emerged during evolution. In principle, DPD1 alone can degrade orgDNA given their heterogeneity, as advocated by Bendich: many orgDNAs are nicked, linearized and have a free 3' end [10,61]. Whether algae or mosses have other types of exonucleases remains elusive, although the salvage function of orgDNAs was postulated earlier for *Chlamydomonas* [62]. TREX1 is a mammal DPD1 homologue [63], which has been shown to be associated with inflammatory disease. Unlike TREX1, which degrades foreign pathogenic DNA, DPD1 has evolved to degrade endogenous DNA for salvage. In agriculture, the use of excess N and P fertilizers has drawn considerable attention, owing to the fact that over-fertilization of crop

fields disturbs the environment, and there is concern over whether the mining of P fertilizers will compromise their availability in the future. Our findings highlight orgDNA as a potential source of P storage, and future engineering for the efficient use of P in crop production.

Methods

Arabidopsis growth conditions and sampling

Arabidopsis thaliana ecotype Columbia (Col) was used as the control throughout this study. *dpd1* mutants (*dpd1-1* and *dpd1-5*) and a G31 transgenic line (*dpd1-1* complemented with the *DPD1* genomic sequence) were described previously [22]. For growing plants, surface-sterilized seeds were placed on 0.8% (w/v) agar plates supplemented with MS medium (Sigma) and 1% (w/v) sucrose for 3 days at 4°C, followed by further growth in MS plates for 18 days at 23°C, at a photoperiod of 10 h light and 14 h darkness. Seedlings were then transplanted to soil and were grown for a further 4–5 weeks. Dark-induced leaf senescence was induced in these mature plants, from which we excised all leaves. We placed the leaves in darkness in a sealed chamber containing wet paper to maintain humidity.

Hydroponic culture

Hydroponic culture of *Arabidopsis* plants was performed as described by Conn et al. [30]with a slight modification: the device used in the culture is shown in Supplementary Fig. 8 along with a detailed description in the legend. We used 1/4 MS medium as the hydroponic medium. Sterilized and cold-treated seeds were germinated on top of 1.5-mL microtubes immersed with 1/4 MS liquid medium (rack culture). After continuous growth for 1 month, whole plants with the microtubes were transferred and plugged into a new 15-mL tube filled with 1/4 MS media (tube culture). Growth was conducted in P- or N-depleted conditions by replacing the medium with medium lacking the corresponding elements 10 days after initiating tube culture. We prepared medium lacking potassium dihydrogen phosphate for -P, and lacking ammonium nitrate and potassium nitrate for -N. Hydroponic culture medium was exchanged with fresh medium every week. Phenotypes and responses to -P or -N deprivation were examined two week after plants were subjected to nutrient deprivation.

Poplar sampling

Periodic sampling of leaves from a white poplar tree (located at Uji Campus, Kyoto University, 34°91'N, 135°80'E, altitude 24 m above sea level, see Supplementary Fig. 12) was conducted during April–November in 2015 and 2016. Sampling was done every month between 13:30

and 14:30. Leaves in the area between 1.0 and 2.5 m from the ground were collected randomly. For each sampling, three sets were prepared, consisting of five leaves, which were subjected to RNA isolation followed by qRT-PCR. Meteorological data were acquired from the database of the Japan Meteorological Agency (http://www.jma.go.jp/jma/menu/menureport.html).

For sampling of leaves from a shortened seasonal cycle system in growth chambers, poplar plants were cultivated initially from potted cuttings (shoots with five leaves at a height of 10 cm) with subsequent incubation at Stage 1 (1 month at 25°C in a 14 h/10 h light/dark cycle), Stage 2 (1 month at 15°C in an 8 h/16 h light/dark cycle) and Stage 3 (2–3 months at 5°C in an 8 h/16 h light/dark cycle). Stages respectively mimic spring/summer, autumn and winter in natural field conditions. Other growth conditions were similar to those reported previously (*26*). For sampling, fifth to seventh leaves from apical meristems on the respective plants were collected. Three sets were prepared and subjected to qRT-PCR.

PCR analysis

For studies of *Arabidopsis*, total DNA was isolated as described previously. For qPCR of organelle genes, primers were designed as listed in Supplementary Table 9. The reactions were performed using a kit (Thunderbird SYBR qPCR Mix; Toyobo Co. Ltd.) and Light Cycler 2.0 software (Roche Diagnostics Corp.) with 40 cycles of denaturation (95°C for 5 s) and extension (60°C for 30 s). Quantitative data were obtained from at least three biological replicates and were analyzed using LightCycler version 4.0 software (Roche Diagnostics Corp.). To normalize qPCR data from orgDNA over nuclear DNA, *DPD1* was used as a control of single-copy nuclear DNA, except that *18S rRNA* was used in Fig. 2a to follow Zoschke et al.[13] (see corresponding figure legends). For studies on *Populus*, we conducted the same experiment as described above, but the primers were designed specifically based on the whole genome sequence of *Populus trichocarpa* (taxid: 3694, Phytozome 12, ver. 3.1) for nuclear genes, chloroplast genome sequence of *Populus alba* (taxid: 43335, Accession: AP008956) for chloroplast genes, and mitochondrial genome sequence of *Populus tremula* (taxid: 113636, Accession: KT337313) for mitochondrial genes. To minimize the amplification of mtDNA or ptDNA sequences included in the nuclear genome, we selected *rpoC1* for ptDNA, and *matR* and *cox3* for mtDNA as a reference. As a control nuclear gene, popular *CAD* gene (Potri.009G095800.1) was selected as a single-copy gene.

For qRT-PCR, total RNA was isolated using an RNeasy Plant Mini Kit (Qiagen), followed by reverse transcriptase and PCR reactions with a ReverTra Ace qPCR RT Kit (Toyobo Co. Ltd.) in accordance with the manufacturer's instructions. For *Arabidopsis*, we used Histone

variant gene *H3.3* as an internal control, as described previously (*16*). For *P. alba*, we used *ACTIN2* (Potri.001G309500.1) as an internal control, to measure the expression levels of *DPD1* (Potri.005G020600.1), *SAG12* (Potri.004G055900.1) and *SGR1* (Potri.003G119600.1).

For digital PCR, a QuantStudio 3D Digital PCR System (Thermo Fisher Scientific Inc.) was used. DNAs were labeled using the Taqman probe method with primers designed accordingly (Supplementary Table 9). We used *PsbA* and *DPD1* to measure the respective levels of cpDNA (FAM labeled) and nuclear DNA (VIC labeled), and adopted 40 cycles of denaturation (98°C for 30 s) and extension (60°C for 2 min) for the PCR reaction. Post-reaction chips were subjected to a QuantStudio 3D digital PCR system. DNA levels were quantified using AnalysisSuite Cloud Software.

All primers used for PCR analyses in this study are listed in Supplementary Table 9, with the accession numbers of the corresponding genes. All quantitative data included at least three biological replicates and are presented with SD in the graphs (statistical analysis is indicated in the corresponding figure legends).

Nuclease assay

The recombinant DPD1-His protein was purified as described previously [22] with a slight modification. Overexpression of proteins was conducted at 28°C. Ni^{2+}-affinity purification was performed with Ni-NTA agarose (GE Healthcare). After purification, the imidazole-containing buffer was exchanged for 2× DPD1 storage buffer (100 mM Tris-HCl [pH 7.5], 200 mM NaCl) using a gel filtration column midiTrap G-25 (GE Healthcare). The obtained fractions containing the desired protein were subjected to centrifugation with AmiconUltra-4 (10K) (Millipore Corp.) to concentrate the recombinant protein to >2.0 μg μL^{-1}. The protein solution was diluted to adjust the concentration to 2.0 μg μL^{-1}, and was subsequently mixed with an equal amount of glycerol to make a 1.0 μg μL^{-1} stock solution. Stock solution aliquots were stored at -30°C until use. Either aliquots of soluble proteins extracted from *E. coli* cells or purified recombinant proteins were solubilized by incubation at 75°C for 5 min in the presence of 2% SDS and 0.1 M DTT. The protein samples were centrifuged for 1 min at >20,000 × *g* and were then subjected to SDS-PAGE with 12.5% (w/v) polyacrylamide gels. The proteins in the gel were subsequently visualized by staining (CBB Stain ONE; Nacalai Tesque Inc.).

For the in vitro nuclease assay, we used 6-FAM-labeled oligonucleotides purchased from Hokkaido System Science as substrates. Oligonucleotides of all types (dsDNA, ssDNA and ssRNA) were designed based on the sequence (5′-CGAACACATACTTCACAAGC-3′) derived from one primer used earlier for amplifying a ptDNA fragment (*ndhI* gene). The nuclease assay was performed in a 12.5 μL reaction mixture that consisted of 40 mM Tris-HCl

(pH 7.5), 2 mM $MgCl_2$, 1.6 μM oligonucleotides and 17.5–175 ng of purified DPD1-His protein. Each reaction was terminated by the immediate addition of stopping buffer (1% [w/v] SDS, 50% [v/v] glycerol, 0.05% [w/v] bromophenol blue). After each reaction, the digestion products were separated electrophoretically on 20% (w/v, acrylamide: bis = 29: 1) polyacrylamide gels. For double-stranded DNA, reaction mixtures with no treatment were loaded on a polyacrylamide gel. Reaction mixtures containing single-stranded DNA or RNA were supplemented with an equal amount of denaturing buffer (TBE buffer containing 10 M urea, 20% [v/v] glycerol and 0.1% [w/v] bromophenol blue) and were then heated at 65°C for 5 min. Subsequently, the samples were subjected to denaturing polyacrylamide gel electrophoresis in the presence of 7 M urea. The separated fragments were detected using an image analyzer (LAS4000; Fuji).

Cytological observation

For observing DNA with 4,6-diamido-2-phenylindole (DAPI), leaves were simultaneously fixed and stained with 1 μg/mL DAPI（3% [w/v] glutaraldehyde). The leaves were observed directly using a microscope (BX61; Olympus Optical Co. Ltd.) equipped with a disc scan unit. When necessary, sections were prepared using a vibratome VT 1200S (Leica Biosystems) with samples embedded in either 4% (w/v) gelatin or 1.5% (w/v) agarose, setting blade speed 0.4 mm/s, blade vibration 1.5 mm, thickness 70–100 μm and blade angle of 12–15°.

Phylogenetic analysis

Protein sequences homologous to DPD1 were obtained from the PLAZA database (https://bioinformatics.psb.ugent.be/plaza/). Multiple alignment of the extracted homologues was performed using MUSCLE software with the MEGA7 database. An unrooted tree was constructed using the Maximum Likelihood method based on the JTT matrix-based model with the default settings in MEGA7.

Photosynthetic activity measurement

Photosynthetic activity of Col and *dpd1* leaves of plants grown in soil was measured as the transpiration rate (LI-6400XT; Li-Cor Inc.). The same leaves were subjected to measurement to estimate the decline in photosynthetic activity at 1 and 2 weeks after the initial measurements. CO_2-dependent photosynthesis curves were obtained at a light intensity of 1,000 μmol m^{-2} s^{-1}. For each measurement, the relative moisture of the chamber was adjusted to 60–70%.

Arabidopsis RNA seq analysis

For RNA seq in Arabidopsis, total RNA was isolated from leaves either in P depletion or control conditions as described above. RNA sequencing was conducted using a HiSeq 2500 or 4000 Illumina sequencing platform and outsourced (Macrogen Corp. Japan), including DNA library preparation using a TruSeq RNA sample Prep Kit v2 and sequencing reaction with a TruSeq rapid SBS kit, Truseq SBS Kit v4, or TruSeq 3000 4000 SBS Kit v3. Sequences were obtained as pair-end reads. At least four billion reads were obtained for each sample (n=3). Mapping of the obtained sequences was performed using the Quas/R package. The gene expression levels were detected by edge/R after normalization with the TCC package. Volcano plots were constructed using the ggplot2/R package with the dataset of all differentially expressed genes (Supplementary Table 1 and Supplementary Table 2 for -P, and Supplementary Table 5 and Supplementary Table 6 for -N). Box plots were constructed using boxplot and beeswarm/R packages with the dataset of the selected genes (Supplementary Table 3 and Supplementary Table 4 for -P, and Supplementary Table 7 and Supplementary Table 8 for -N), which was reported earlier as P-responding [33] or as N-responding [32,34], respectively.

Measurement of total phosphorus contents

Plants grown in hydroponic culture, with 1/4 MS or in -P conditions, were subjected to P measurement. Before P deprivation, all leaves were marked as lower leaves, whereas newly emerged leaves in -P condition (2 weeks) were designated as upper leaves. Samples (n=6) were dried in an oven at 60°C for at least 1 day. Dried samples were then digested with 60% (w/v) nitric acid at temperatures as high as 180°C. The concentration of P in the digested solution was ascertained using ICP-mass spectrometry (7500CX; Agilent Technologies Inc.).

Reporting summary

Further information on experimental design is available in the Nature Research Reporting Summary linked to this article.

Data availability

Accession numbers of the genes used in this study are listed in Supplementary Table 9. Precise p values calculated by statistical tests in this study are listed in Supplementary Table 10. The raw data used to construct graphs in this study are presented as Supplementary Dataset. The raw transcriptomic data are deposited in the DDBJ with the accession number

575 DRA007138, under the BioProject with the accession number PRJDB7233. All transcriptomic
576 data used in Fig. 5, Supplementary Figs. 10 and 11 are available in Supplementary tables
577 1-8.
578

References

1 Dyall, S. D., Brown, M. T. & Johnson, P. J. Ancient invasions: from endosymbionts to organelles. *Science* **304**, 253-257 (2004).

2 Gray, M. W. Evolution of organellar genomes. *Curr Opin Genet Dev* **9**, 678-687 (1999).

3 Sugiura, M. History of chloroplast genomics. *Photosynth Res* **76**, 371-377 (2003).

4 Wallace, D. C. Why do we still have a maternally inherited mitochondrial DNA? Insights from evolutionary medicine. *Annu Rev Biochem* **76**, 781-821 (2007).

5 Sato, S., Nakamura, Y., Kaneko, T., Asamizu, E. & Tabata, S. Complete structure of the chloroplast genome of Arabidopsis thaliana. *DNA Res* **6**, 283-290 (1999).

6 Jarvis, P. & Lopez-Juez, E. Biogenesis and homeostasis of chloroplasts and other plastids. *Nat Rev Mol Cell Biol* **14**, 787-802 (2013).

7 Sakamoto, W., Miyagishima, S. Y. & Jarvis, P. Chloroplast biogenesis: control of plastid development, protein import, division and inheritance. *Arabidopsis Book* **6**, e0110 (2008).

8 Gualberto, J. M. & Newton, K. J. Plant Mitochondrial Genomes: Dynamics and Mechanisms of Mutation. *Annu Rev Plant Biol* **68**, 225-252 (2017).

9 Marechal, A. & Brisson, N. Recombination and the maintenance of plant organelle genome stability. *New Phytol* **186**, 299-317 (2010).

10 Oldenburg, D. J. & Bendich, A. J. DNA maintenance in plastids and mitochondria of plants. *Front Plant Sci* **6**, 883 (2015).

11 Rauwolf, U., Golczyk, H., Greiner, S. & Herrmann, R. G. Variable amounts of DNA related to the size of chloroplasts III. Biochemical determinations of DNA amounts per organelle. *Molecular genetics and genomics : Mol Genet Genom* **283**, 35-47 (2010).

12 Fujie, M., Kuroiwa, H., Kawano, S., Mutoh, S. & Kuroiwa, T. Behavior of oeganelles and their nucleoids in the shoot apical meristem during leaf development in *Arabidopsis thaliana* L. *Planta* **194**, 395-405 (1994).

13 Zoschke, R., Liere, K. & Borner, T. From seedling to mature plant: arabidopsis plastidial genome copy number, RNA accumulation and transcription are differentially regulated during leaf development. *Plant J* **50**, 710-722 (2007).

14 Dean, C. & Leech, R. M. Genome Expression during Normal Leaf Development : I. Cellular and chloroplast numbers and DNA, RNA, and protein levels in tissues of different ages within a seven-day-old wheat leaf. *Plant Physiol* **69**, 904-910 (1982).

15 Veneklaas, E. J. *et al.* Opportunities for improving phosphorus-use efficiency in crop plants. *New Phytol***195**, 306-320 (2012).

16 Golczyk, H. *et al.* Chloroplast DNA in mature and senescing leaves: a reappraisal. *Plant Cell* **26**, 847-854 (2014).
17 Oldenburg, D. J., Rowan, B. A., Kumar, R. A. & Bendich, A. J. On the fate of plastid DNA molecules during leaf development: response to the Golczyk et al. Commentary. *Plant Cell* **26**, 855-861 (2014).
18 Sato, M. & Sato, K. Maternal inheritance of mitochondrial DNA by diverse mechanisms to eliminate paternal mitochondrial DNA. *Biochim Biophys Acta* **1833**, 1979-1984 (2013).
19 Kuroiwa, T. Review of cytological studies on cellular and molecular mechanisms of uniparental (maternal or paternal) inheritance of plastid and mitochondrial genomes induced by active digestion of organelle nuclei (nucleoids). *J Plant Res* **123**, 207-230 (2010).
20 Zhou, Q. *et al.* Mitochondrial endonuclease G mediates breakdown of paternal mitochondria upon fertilization. *Science* **353** (2016).
21 Nishimura, Y. *et al.* An mt(+) gamete-specific nuclease that targets mt(-) chloroplasts during sexual reproduction in *C. reinhardtii*. *Genes Dev* **16**, 1116-1128 (2002).
22 Matsushima, R. *et al.* A conserved, Mg(2)+-dependent exonuclease degrades organelle DNA during Arabidopsis pollen development. *Plant Cell* **23**, 1608-1624 (2011).
23 Sakamoto, W. & Takami, T. Nucleases in higher plants and their possible involvement in DNA degradation during leaf senescence. *J Exp Bot* **65**, 3835-3843 (2014).
24 Portis, A. R., Jr. & Heldt, H. W. Light-dependent changes of the Mg2+ concentration in the stroma in relation to the Mg^{2+} dependency of CO2 fixation in intact chloroplasts. *Biochim Biophys Acta* **449**, 434-436 (1976).
25 Parent, J. S., Lepage, E. & Brisson, N. Divergent roles for the two PolI-like organelle DNA polymerases of Arabidopsis. *Plant Physiol* **156**, 254-262 (2011).
26 Moriyama, T. & Sato, N. Enzymes involved in organellar DNA replication in photosynthetic eukaryotes. *Front Plant Sci* **5**, 480 (2014).
27 Wang, D. Y. *et al.* The levels of male gametic mitochondrial DNA are highly regulated in angiosperms with regard to mitochondrial inheritance. *Plant Cell* **22**, 2402-2416 (2010).
28 Preuten, T. *et al.* Fewer genes than organelles: extremely low and variable gene copy numbers in mitochondria of somatic plant cells. *Plant J* **64**, 948-959 (2010).
29 Arimura, S. I. Fission and fusion of plant mitochondria, and genome maintenance. *Plant Physiol* **176**, 152-161 (2018).

30 Conn, S. J. *et al.* Protocol: optimising hydroponic growth systems for nutritional and physiological analysis of Arabidopsis thaliana and other plants. *Plant Methods* **9**, 4 (2013).

31 Rubio, V. *et al.* A conserved MYB transcription factor involved in phosphate starvation signaling both in vascular plants and in unicellular algae. *Genes Dev* **15**, 2122-2133 (2001).

32 Krapp, A. *et al.* Arabidopsis roots and shoots show distinct temporal adaptation patterns toward nitrogen starvation. *Plant Physiol* **157**, 1255-1282 (2011).

33 Castrillo, G. *et al.* Root microbiota drive direct integration of phosphate stress and immunity. *Nature* **543** (2017).

34 Peng, M., Bi, Y. M., Zhu, T. & Rothstein, S. J. Genome-wide analysis of Arabidopsis responsive transcriptome to nitrogen limitation and its regulation by the ubiquitin ligase gene NLA. *Plant Mol Biol* **65**, 775-797 (2007).

35 Keskitalo, J., Bergquist, G., Gardestrom, P. & Jansson, S. A cellular timetable of autumn senescence. *Plant Physiol* **139**, 1635-1648 (2005).

36 Kurita, Y. *et al.* Establishment of a shortened annual cycle system; a tool for the analysis of annual re-translocation of phosphorus in the deciduous woody plant (Populus alba L.). *J Plant Res* **127**, 545-551, doi:10.1007/s10265-014-0634-2 (2014).

37 Kurita, Y. *et al.* Inositol Hexakis Phosphate is the Seasonal Phosphorus Reservoir in the Deciduous Woody Plant Populus alba L. *Plant Cell Physiol* **58**, 1477-1485 (2017).

38 Fulgosi, H. *et al.* Degradation of chloroplast DNA during natural senescence of maple leaves. *Tree Physiol* **32**, 346-354 (2012).

39 Sodmergen, Kawano, S., Tano, S. & Kuroiwa, T. Preferential digestion of chloroplast nuclei (nucleoids) during senescence of the coleoptile of *Oryza sativa*. *Protoplasma* **152**, 65-68 (1989).

40 Inada, N., Sakai, A., Kuroiwa, H. & Kuroiwa, T. Three-dimensional analysis of the senescence program in rice (*Oryza sativa* L.) coleoptiles. *Planta* **206**, 585-597 (1998).

41 Sakamoto, W. & Takami, T. Chloroplast DNA Dynamics: Copy Number, Quality Control and Degradation. *Plant Cell Physiol* **59**, 1120-1127 (2018).

42 Zhang, Q., Liu, Y. & Sodmergen. Examination of the cytoplasmic DNA in male reproductive cells to determine the potential for cytoplasmic inheritance in 295 angiosperm species. *Plant Cell Physiol* **44**, 941-951 (2003).

43 Mogensen, H. L. The hows and whys of cytoplasmic inheritance in seed plants. *Am. J. Bot.* **83**, 383-404 (1996).

44 Corriveau, J. L. & Coleman, A. W. Rapid screening method to detect potential

biparental inheritance of plastid DNA and results for over 200 angiosperm species. *Am. J. Bot.* **75**, 1443-1458 (1988).

45 Tang, L. Y., Matsushima, R. & Sakamoto, W. Mutations defective in ribonucleotide reductase activity interfere with pollen plastid DNA degradation mediated by DPD1 exonuclease. *Plant J* **70**, 637-649 (2012).

46 Lim, P. O., Kim, H. J. & Nam, H. G. Leaf senescence. *Annu Rev Plant Biol* **58**, 115-136 (2007).

47 Gregersen, P. L., Culetic, A., Boschian, L. & Krupinska, K. Plant senescence and crop productivity. *Plant Mol Biol* **82**, 603-622 (2013).

48 Krupinska, K. in *The structure and function od plastids* (eds R.R. Wise & J.K. Hoober) 433-449 (Springer, 2006).

49 Makino, A. & Osmond, B. Effects of Nitrogen Nutrition on Nitrogen Partitioning between Chloroplasts and Mitochondria in Pea and Wheat. *Plant Physiol* **96**, 355-362 (1991).

50 Smith, D. W., Fontenot, E. B., Zhahraeifard, S. & DiTusa, S. F. Molecular components that drive phophorus-remobilization during leaf senescence. *Annu Plant Rev* **48**, 159-186 (2015).

51 Stigter, K. A. & Plaxton, W. C. Molecular Mechanisms of Phosphorus Metabolism and Transport during Leaf Senescence. *Plants (Basel)* **4**, 773-798 (2015).

52 Robinson, W. D., Carson, I., Ying, S., Ellis, K. & Plaxton, W. C. Eliminating the purple acid phosphatase AtPAP26 in Arabidopsis thaliana delays leaf senescence and impairs phosphorus remobilization. *New Phytol* **196**, 1024-1029 (2012).

53 Bariola, P. A., MacIntosh, G. C. & Green, P. J. Regulation of S-like ribonuclease levels in Arabidopsis. Antisense inhibition of RNS1 or RNS2 elevates anthocyanin accumulation. *Plant Physiol* **119**, 331-342 (1999).

54 Perez-Amador, M. A. *et al.* Identification of BFN1, a bifunctional nuclease induced during leaf and stem senescence in Arabidopsis. *Plant Physiol* **122**, 169-180 (2000).

55 Matallana-Ramirez, L. P. *et al.* NAC transcription factor ORE1 and senescence-induced BIFUNCTIONAL NUCLEASE1 (BFN1) constitute a regulatory cascade in Arabidopsis. *Mol Plant* **6**, 1432-1452 (2013).

56 Liere, K. & Borner, T. in *Plastid development in leaves during growth and senescence, Advances in Photosynthesis and Respiration* Vol. 36 (eds B. Biswal, K. Krupinska, & U.C. Biswal) 215-237 (Springer, 2013).

57 Chiou, T. J. & Lin, S. I. Signaling network in sensing phosphate availability in plants. *Annu Rev Plant Biol* **62**, 185-206 (2011).

58 Versaw, W. K. & Garcia, L. R. Intracellular transport and compartmentation of phosphate in plants. *Curr Opin Plant Biol* **39**, 25-30 (2017).

59 Liu, T. Y., Lin, W. Y., Huang, T. K. & Chiou, T. J. MicroRNA-mediated surveillance of phosphate transporters on the move. *Trends Plant Sci* **19**, 647-655 (2014).

60 Ishida, H., Izumi, M., Wada, S. & Makino, A. Roles of autophagy in chloroplast recycling. *Biochim Biophys Acta* **1837**, 512-521 (2014).

61 Bendich, A. J. Circular chloroplast chromosomes: the grand illusion. *Plant Cell* **16**, 1661-1666 (2004).

62 Sears, B. B. & VanWinkle-Swift, K. The salvage/turnover/repair (STOR) model for uniparental inheritance in Chlamydomonas: DNA as a source of sustenance. *J Hered* **85**, 366-376 (1994).

63 Yang, Y. G., Lindahl, T. & Barnes, D. E. Trex1 exonuclease degrades ssDNA to prevent chronic checkpoint activation and autoimmune disease. *Cell* **131**, 873-886 (2007).

ACKNOWLEDGEMENTS

We thank Rie Hijiya (Institute of Plant Science and Resources, Okayama University) for technical support and Dr. Hiromi Kanegae (Graduate School of Agricultural and Life Sciences, The University of Tokyo) for assisting mtDNA sequence alignment in *Populus* species, and Dr. Keiichi Baba (Research Institute for Sustainable Humanosphere, Kyoto University) for supporting poplar leaf sampling. This work was supported by KAKENHI grants from JSPS (16H06554 and 17H03699 to W.S.) and from the Oohara Foundation (to W.S).

AUTHOR INFORMATION

Affiliations

Institute of Plant Science and Resources, Okayama University, Kurashiki, Japan

Tsuneaki Takami, Norikazu Ohnishi & Wataru Sakamoto

Department of Biology, Graduate School of Science, Kobe University, Kobe, Japan

Yuko Kurita, Shoko Iwamura, Miwa Ohnishi & Tetsuro Mimura

Graduate School of Science, Hiroshima University, Higashi-Hiroshima, Japan

Makoto Kusaba

Contributions

W.S. designed the project. T.T. performed all qPCR and qRT-PCR measurements for various environments, in addition to photosynthetic activity measurements and RNA seq analysis. N.O. performed nuclease assays. Y.K., S.I., M.O. and T.M. prepared poplar samples and conducted primary work related to poplar. T.T., M.K. and W.S. analyzed the data. W.S. wrote the manuscript with consultation among all coauthors.

Competing interests

The authors declare no competing interests.

SUPPLEMENTARY INFORMATION

Supplementary Figures 1–15

Supplementary Tables 1–8

Supplementary Table 9

Supplementary Table 10

Supplementary Dataset

Reporting Summary

Figure legends

Fig. 1 | Exonuclease activity of DPD1. a, Schematic representation of the *DPD1* construct used for this study (top), and Coomassie-stained SDS-PAGE gel showing the induction of DPD1 fusion proteins (left) and fusion proteins purified using an Ni-NTA agarose column (right). The control sample without induction (C) and IPTG-induced samples (I) are indicated. M, molecular weight markers. **b,** In vitro nuclease assay of DPD1-His using 20-mer double-stranded DNA (dsDNA), single-stranded DNA (ssDNA) or ssRNA as substrate. Arrowheads indicate the positions of the substrates. **c,** Non-denaturing 20% polyacrylamide gel electrophoresis demonstrating Mg^{2+} dependence of the nuclease activity. 20-mer ssDNA was used as the substrate (indicated by red arrows). **d,** Denaturing 20% polyacrylamide gel electrophoresis demonstrating 3'-to-5' polarity of the nuclease activity. Either 5′ - or 3′ - end-labeled 20-mer ssDNA was used as a substrate. All nuclease assays were repeated twice with three independent sample preparations.

Fig. 2 | DPD1 is induced by leaf senescence and degrades orgDNA in vivo. a, Decline in cpDNA levels during dark-induced leaf senescence in Col, as estimated by qPCR (*psbA* was used for cpDNA and *18S rRNA* for nuclear DNA). Representative images of senescing leaves on days 0–5 are presented at the top. **b,** Retention of cpDNA in *dpd1* estimated by qPCR (open and closed circles represent *dpd1* and Col, respectively). Chloroplast genes used for qPCR are presented in each graph. The copy number of cpDNA was estimated by normalization with *DPD1*. **c,** Upregulation of *DPD1* transcripts in Col senescing leaves, as estimated by qRT-PCR. **d,** Cytological observation of chloroplasts (chlorophyll autofluorescence, Chl) and cpDNAs (stained with DAPI) in senescing leaves of Col and *dpd1* (after 5 days in darkness). **e,** Estimation of cpDNA copy number in senescing leaves (after 5 days in darkness) of Col, *dpd1*, *polIa2* and *dpd1/polIa2* by qPCR (*psbA*/DPD1, n=3, Student's t-test, two-sided, *P<0.05, **P<0.01, p values shown in Supplementary Table 10). All quantitative data in Fig. 2 were from three biological replicates (Supplementary Dataset) and are shown as mean values with SD error bars.

Fig. 3 | Stay-green phenotype and prolonged leaf longevity in *dpd1*. a, Detached leaves subjected to dark-induced senescence from Col, *dpd1-1* and G31 (transgenic *dpd1-1* complemented by *DPD1*). All detached leaves from the respective plants are aligned from left (younger) to right (older) before dark induction (Day 0) and after 5 days in darkness (Day 5). Representative images from three independent experiments are shown. A similar stay-green

phenotype was observed in *dpd1-5* (Supplementary Fig. S6). **b,** Chlorophyll contents of senescing leaves (ninth-oldest leaves among all leaves subjected to dark induction) from Col (closed) and *dpd1-1* (open) (mean value ± SD, *n*=4 , Dunnett's test, against day 0, two-sided, ***P<0.001, p values shown in Supplementary Table 10). **c,** Retarded decline in transcripts encoded in chloroplasts (*psbA*, *clpP*) and those encoding chloroplast-targeted proteins (*psbO*, *SIG2*), estimated by qRT-PCR (mean value with SD, *n*=3, Dunnett's test, two-sided, *P<0.05, **P<0.01, ***P<0.01, p values shown in Supplementary Table 10). Other transcripts are also indicated in Supplementary Fig. S7. **d,** CO_2-dependent photosynthetic activity of mature leaves from Col and *dpd1-1*, grown in normal conditions with a light intensity of 1,000 μmol m^{-2} s^{-1} (mean value ± SD, *n*=6, Student's-*t* test, two-sided). **e,** Photosynthetic activity as in **d**, but at a fixed CO_2 concentration of 1,100 ppm (mean value ± SD, *n*=6, Dunnett's test, two-sided, against initial measurements). Initial measurements were conducted in mature leaves from Col and *dpd1-1* (black, left bar) with subsequent measurements taken of the same leaves after 1 week (gray, middle bar) and 2 weeks (light gray, right bar). Raw data for all quantitative analyses are shown in Supplementary Dataset.

Fig. 4 | Hydroponic culture of *dpd1* exhibited attenuated P response and reduced fitness in phosphate-deprivation conditions. a, Growth rate of Col (red bars) and *dpd1-1* (blue bars) estimated by the weight of aerial part in standard 1/4 MS conditions, either with standard (1/4) or additional (1/2 and 1) P concentration for 2 weeks (4 biological replicates). Weights are presented as the mean values ±SD (Col 1/4P: 423 ± 78 (*n*=12); *dpd1-1* 1/4P: 259 ± 107 (*n*=15); Col 1/2P: 401 ± 89 (*n*=12); *dpd1-1* 1/2P: 350 ± 103 (*n*=18); Col 1P: 344 ± 126 (*n*=13); *dpd1-1* 1P; 388 ± 72 (*n*=19), FW: fresh weight. **P < 0.01 calculated using Dunnett's test, two-sided, p value shown in Supplementary Table 10). **b,** Leaves from Col, *dpd1* and G31 exposed to -P conditions for 2 weeks (upper panels). Representative images from three independent experiments are shown. Typical symptoms showing purple pigmentation in *dpd1* are indicated by arrowheads. Lower panels depict representative images of a *dpd1* leaf showing anthocyanin accumulation and a young silique showing aborted seed development (arrowheads). **c** and **d,** Estimation of cpDNA copy number by qPCR, in leaves from Col and *dpd1-1* subjected to -P (**c**) or -N (**d**) for 2 weeks. Leaf number (1, 2 and 3) denotes the younger (upper) leaf as Leaf 1, in a plant grown hydroponically for 2 months (mean value ±SD, 3 biological replicates, *n*=3, Dunnett's test, two-sided, against leaf 1, *P<0.05, p value shown in Supplementary Table 10). Examples of leaves used for cpDNA measurement are shown in Supplementary Fig. S8d. **e** Fitness of Col and *dpd1* plants estimated by seed set. Plants grown in normal conditions in soil, in standard hydroponic

culture (1/4 MS), -P in hydroponic culture (-P) and -N in hydroponic culture (-N) are compared by the number of seeds set per silique (n=50, Games-Howell's test, two-sided, *P<0.05, ***P<0.01, p values shown in Supplementary Table 10). Lower whisker, bottom of box, center line of box, top of box and upper whisker shows minimum, lower quartile, median, upper quartile and maximum, respectively. **f,** Remobilization of P from lower to upper leaves (schematically illustrated at the top), grown in either control (1/4 MS, bottom) or -P (top) hydroponic conditions for 2 weeks (see *Methods*). P remobilization was estimated by the ratio of P concentration in upper leaves over that in lower leaves (maen value ±SD, 3 biological replicates, n=6, Student's-t test, two-sided, **P<0.01, p value shown in Supplementary Table 10). Raw data for all quantitative analyses are shown in Supplementary Dataset.

Fig. 5 | RNA seq analysis showing compromised response of *dpd1* to -P. a, Volcano plots showing the genes significantly upregulated in -P conditions (2 weeks) in Col (top) and *dpd1-1* (bottom). Data are obtained from three independent samples. Each dot in the graphs represents a single gene, and those significantly upregulated (FDR <0.05, calculated by Benjamini-Hochberg procedure included in edgeR package) are highlighted in red. **b,** Volcano plots as in **a**, except that the data are from in -N conditions. **c,** Box plot of PSR genes extracted from RNA seq data. 192 PSR genes were detected in our RNA sequence data. Differential expression of these genes (Log_2 fold change) after -P treatment is shown. Each dot represents a single gene. Those showing significant alteration (FDR <0.05) are highlighted in red. Lower whisker, bottom of box, center line of box, top of box and upper whisker shows minimum, lower quartile, median, upper quartile and maximum, respectively. **d,** Box plot as in **c**, except that the data are from genes extracted as responding to -N, in accordance with Krapp et al.[32].

Fig. 6 | CpDNA decline and upregulation of *DPD1* during leaf fall in a deciduous tree *Populus alba*. a, Example of leaf samples from a *P. alba* tree used in this study. Sampling dates are indicated above each panel (in 2014). **b**, Decline in cpDNA copy number estimated by qPCR (*rpoC1* as a reference gene for cpDNA and *CAD* for nuclear DNA; see *Methods*). Mean values with error bars as SE (n=3 for Oct, n=5 for other samples) are shown. **c,** Decline in mtDNA copy number in leaves estimated by qPCR, as in **b**. As a reference gene, *matR* (closed circle) and *cox3* (open circle) are used. **d,** Cytological observation of chloroplasts (chlorophyll autofluorescence, Chl) and cpDNA (DAPI stained) in *P. alba* leaf samples collected in April (top) and October (bottom). Merged images are shown on the left. Results

879 presented in **b**, **c** and **d** are from samples prepared in 2015. Representative images from
880 three independent leaf samples are shown. **e,** Expression of poplar *DPD1* analyzed by
881 qRT-PCR in 2015 (left) and 2016 (right). Mean values with error bars as SE (*n*=3 for Oct 16th,
882 *n*=5 for other samples) are shown. Expression of other genes and meteorological data for
883 each year (irradiance and average temperature) are shown in Supplementary Fig. S14. **f,**
884 Outline of *P. alba* plants grown in a shortened annual-cycle cultivation system using
885 controlled-condition growth chambers. Photographs of representative plants (*n*=3
886 independent samples) used in our study are shown. **g,** Expression of *DPD1* and *SGR*, as in **e**.
887 Mean values with error bars as SE (*n*=3 independent samples) are shown. Raw data for all
888 quantitative analyses are shown in Supplementary Dataset.

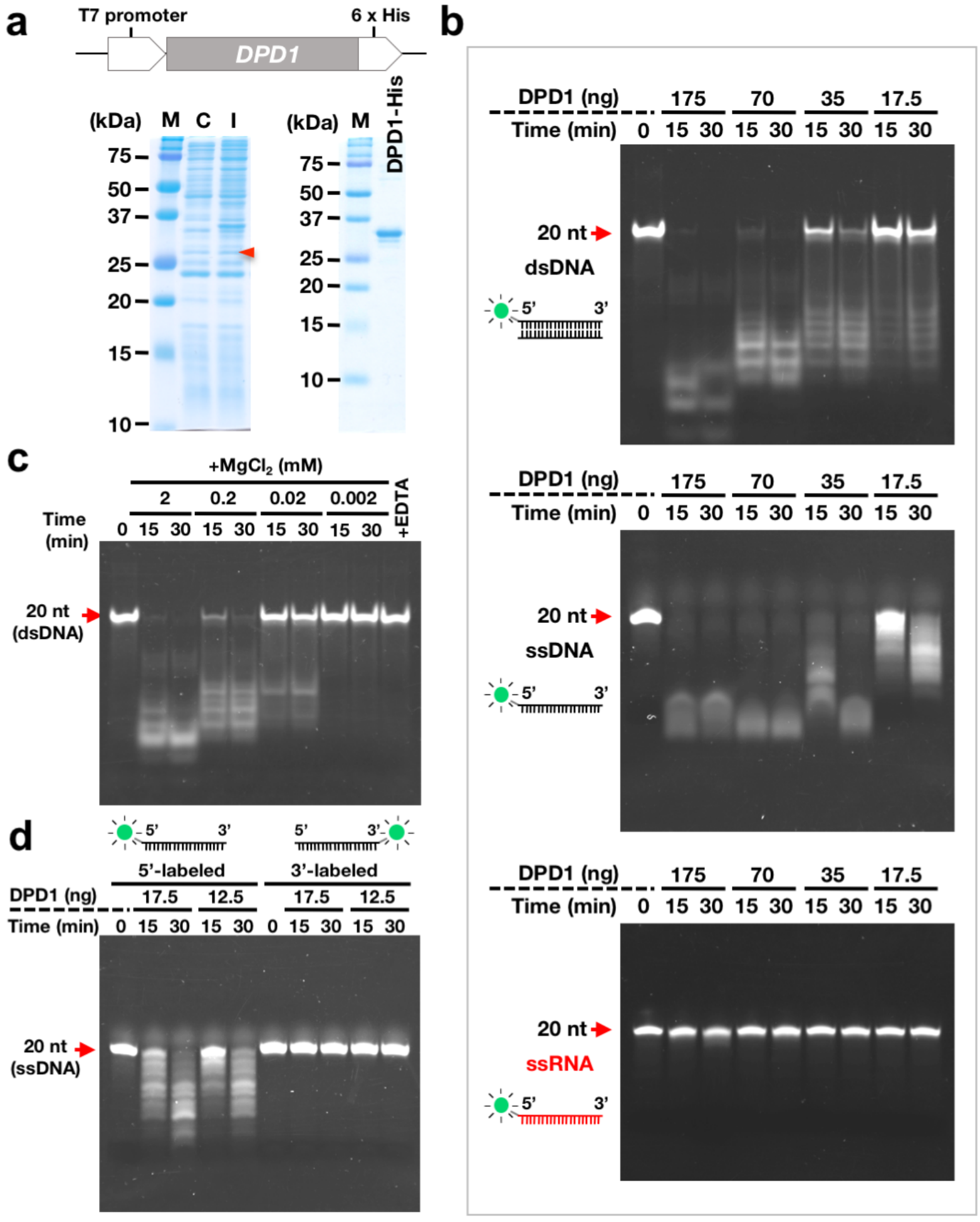
a
T7 promoter
6 x His
DPD1
(kDa) M C I
75
50
37
25
20
15
10
(kDa) M
DPD1-His
b
DPD1 (ng) 175 70 35 17.5
Time (min) 0 15 30 15 30 15 30 15 30
20 nt
dsDNA
5' 3'
DPD1 (ng) 175 70 35 17.5
Time (min) 0 15 30 15 30 15 30 15 30
20 nt
ssDNA
5' 3'
DPD1 (ng) 175 70 35 17.5
Time (min) 0 15 30 15 30 15 30 15 30
20 nt
ssRNA
5' 3'
c
+MgCl2 (mM)
2 0.2 0.02 0.002
Time (min)
0 15 30 15 30 15 30 15 30
+EDTA
20 nt
(dsDNA)
d
5' 3'
5' 3'
5'-labeled
3'-labeled
DPD1 (ng) 17.5 12.5 17.5 12.5
Time (min) 0 15 30 15 30 0 15 30 15 30
20 nt
(ssDNA)

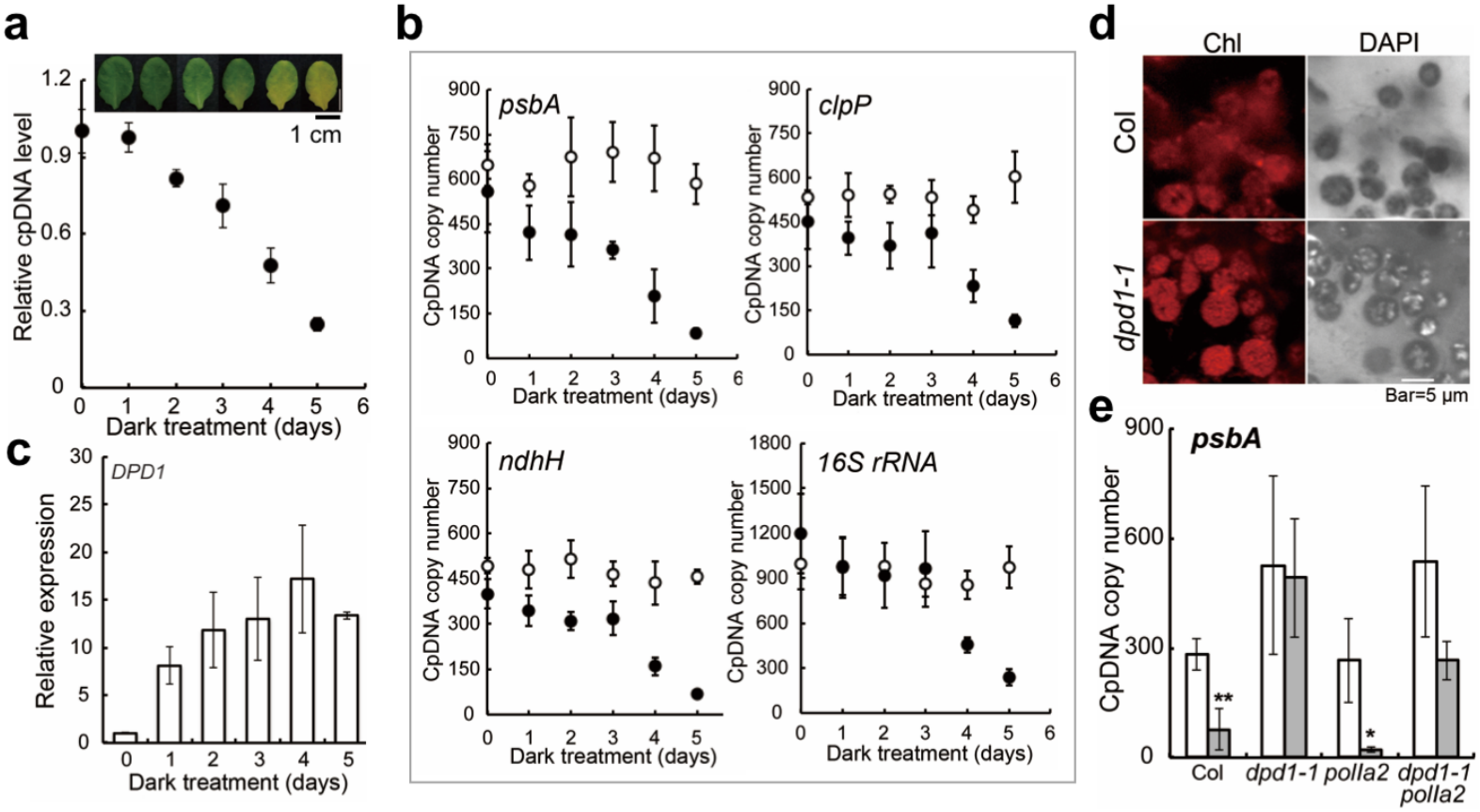
a
1 cm
Relative cpDNA level
Dark treatment (days)
b
psbA
clpP
ndhH
16S rRNA
CpDNA copy number
Dark treatment (days)
c
DPD1
Relative expression
Dark treatment (days)
d
Chl
DAPI
Col
dpd1-1
Bar=5 μm
e
psbA
CpDNA copy number
Col
dpd1-1
polla2
dpd1-1 polla2

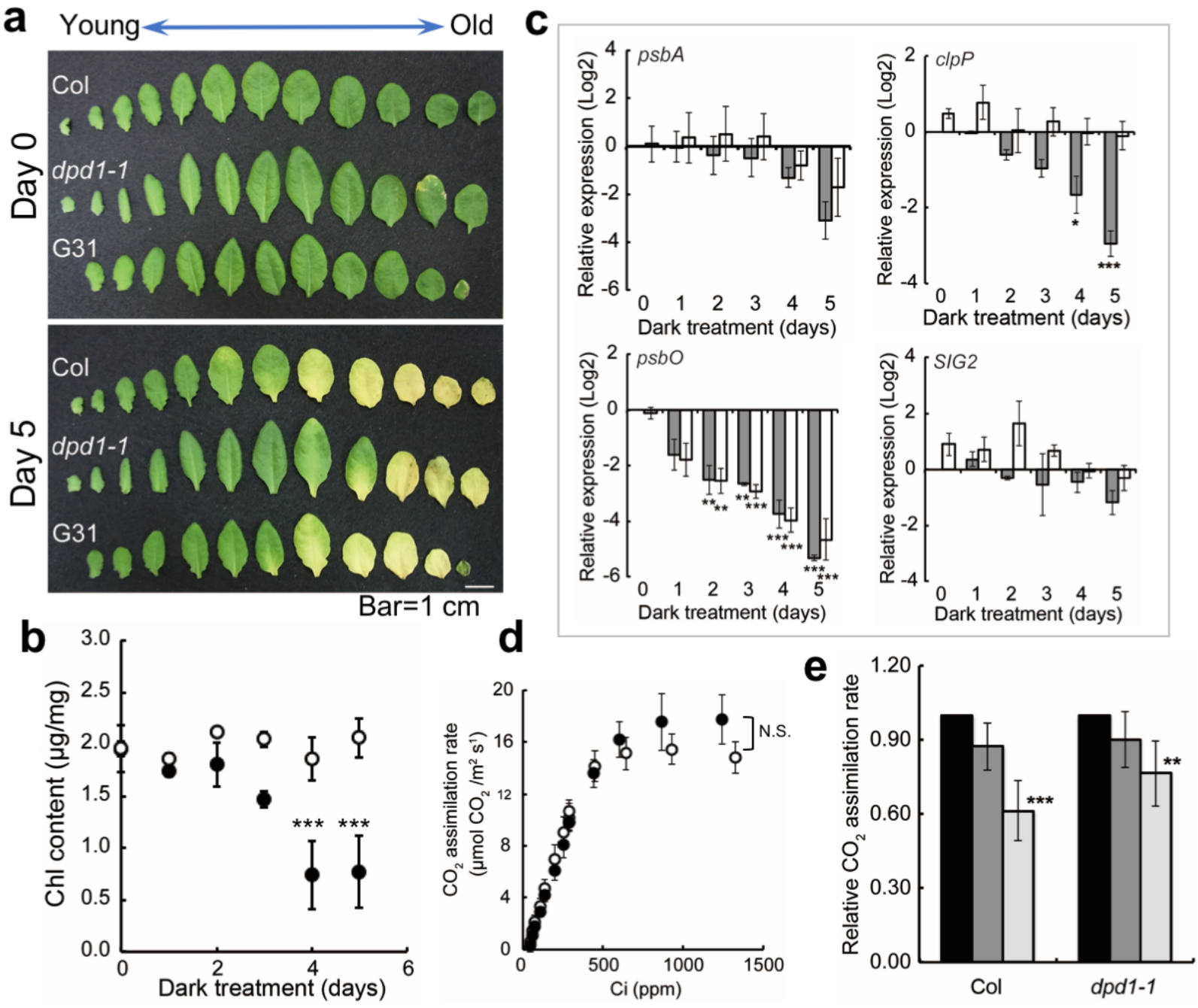
a
Young
Old
Day 0
Day 5
Col
dpd1-1
G31
Bar=1 cm
b
Chl content (μg/mg)
Dark treatment (days)
c
psbA
clpP
psbO
SIG2
Relative expression (Log2)
Dark treatment (days)
d
CO2 assimilation rate (μmol CO2 /m2 s1)
Ci (ppm)
N.S.
e
Relative CO2 assimilation rate
Col
dpd1-1

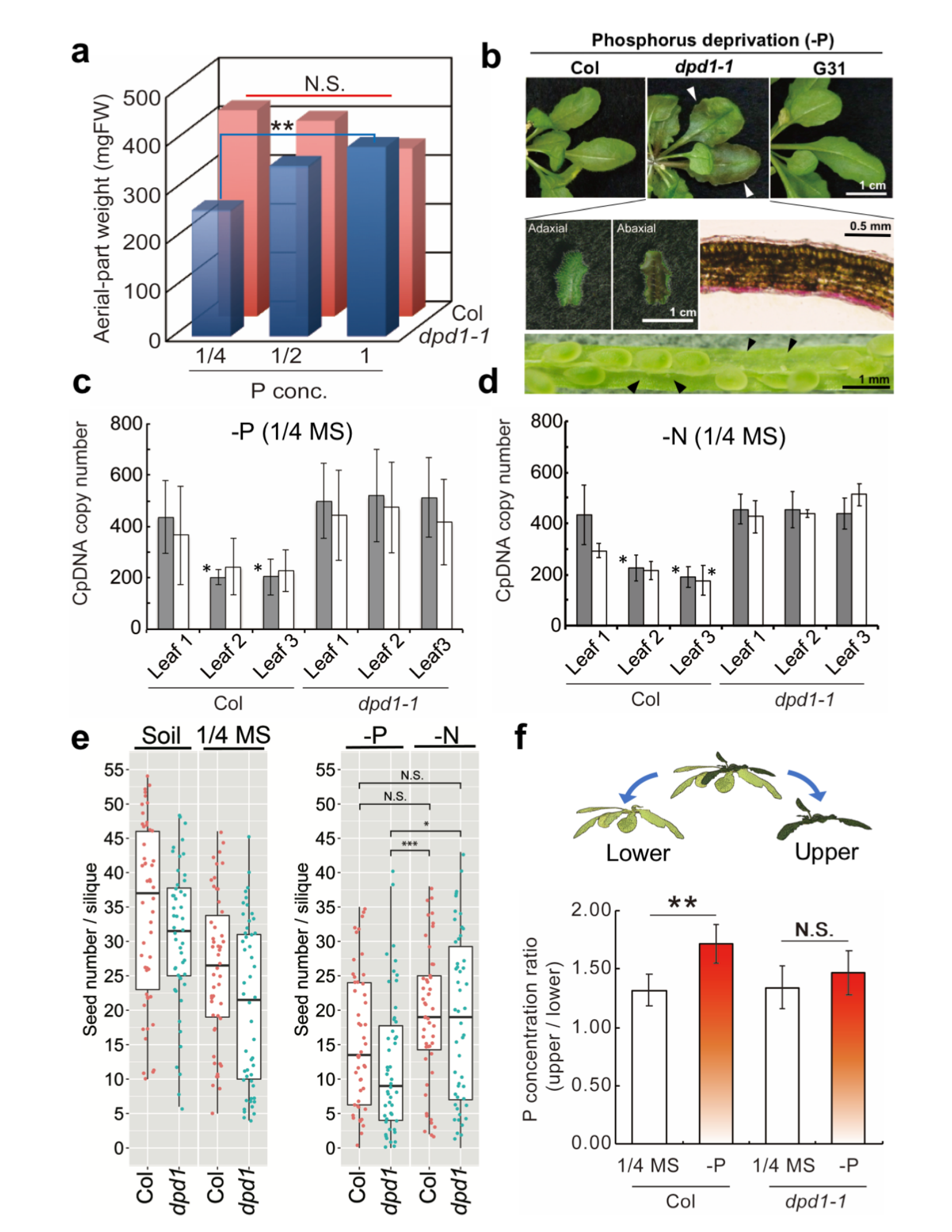
a
Aerial-part weight (mgFW)
500
400
300
200
100
0
N.S.
**
Col
dpd1-1
1/4
1/2
1
P conc.
b
Phosphorus deprivation (-P)
Col
dpd1-1
G31
1 cm
Adaxial
Abaxial
1 cm
0.5 mm
1 mm
c
-P (1/4 MS)
CpDNA copy number
800
600
400
200
0
Leaf 1
Leaf 2
Leaf 3
Leaf 1
Leaf 2
Leaf3
Col
dpd1-1
d
-N (1/4 MS)
CpDNA copy number
800
600
400
200
0
Leaf 1
Leaf 2
Leaf 3
Leaf 1
Leaf 2
Leaf 3
Col
dpd1-1
e
Soil
1/4 MS
-P
-N
Seed number / silique
55
50
45
40
35
30
25
20
15
10
5
0
N.S.
N.S.
*
***
Col
dpd1
Col
dpd1
Col
dpd1
Col
dpd1
f
Lower
Upper
P concentration ratio
(upper / lower)
2.00
1.50
1.00
0.50
0.00
**
N.S.
1/4 MS
-P
1/4 MS
-P
Col
dpd1-1

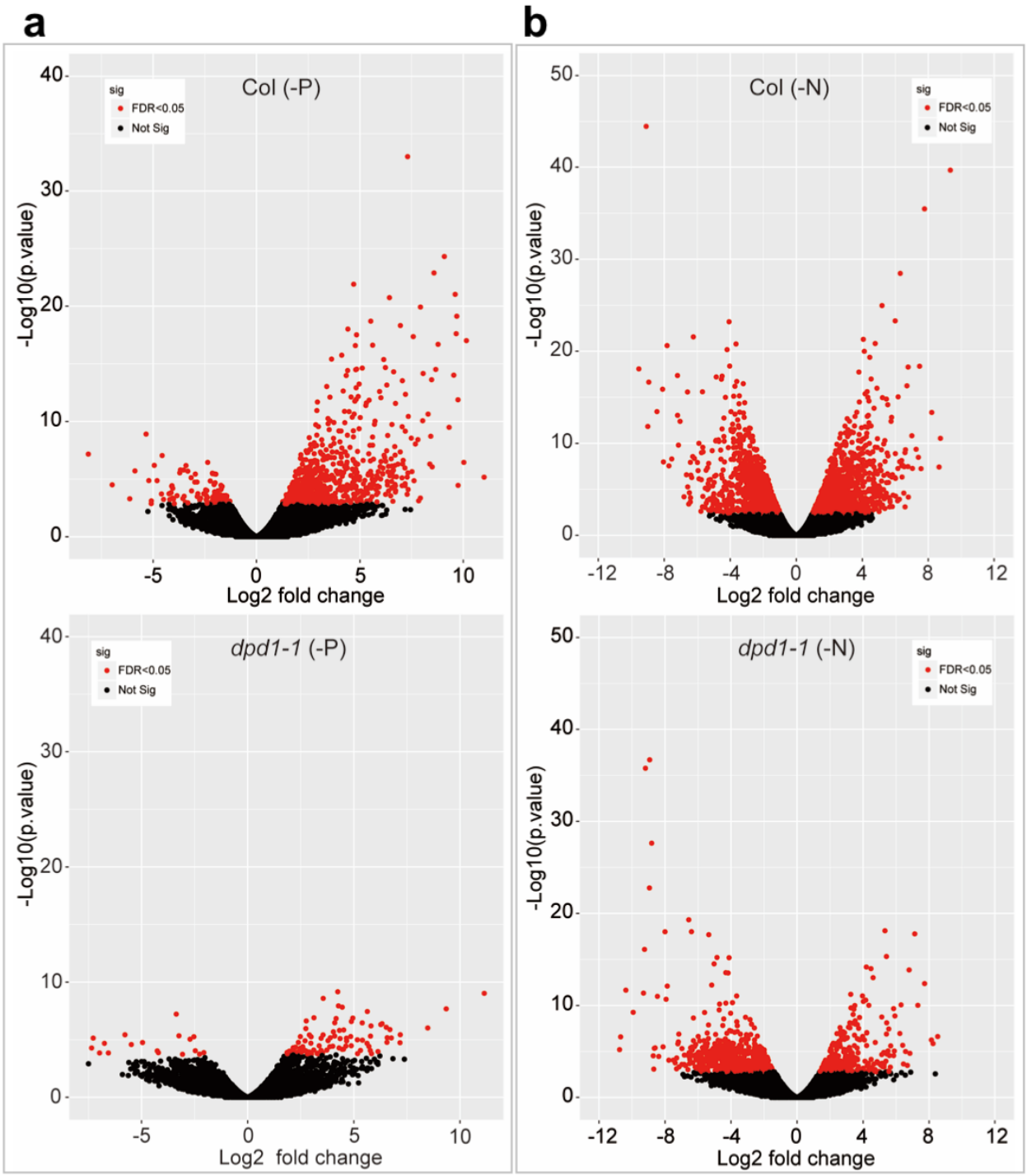
a
Col (-P)
sig
FDR<0.05
Not Sig
-Log10(p.value)
Log2 fold change
dpd1-1 (-P)
Log2 fold change
b
Col (-N)
dpd1-1 (-N)
c
-P
Log2 fold change
Col
dpd1-1
d
-N

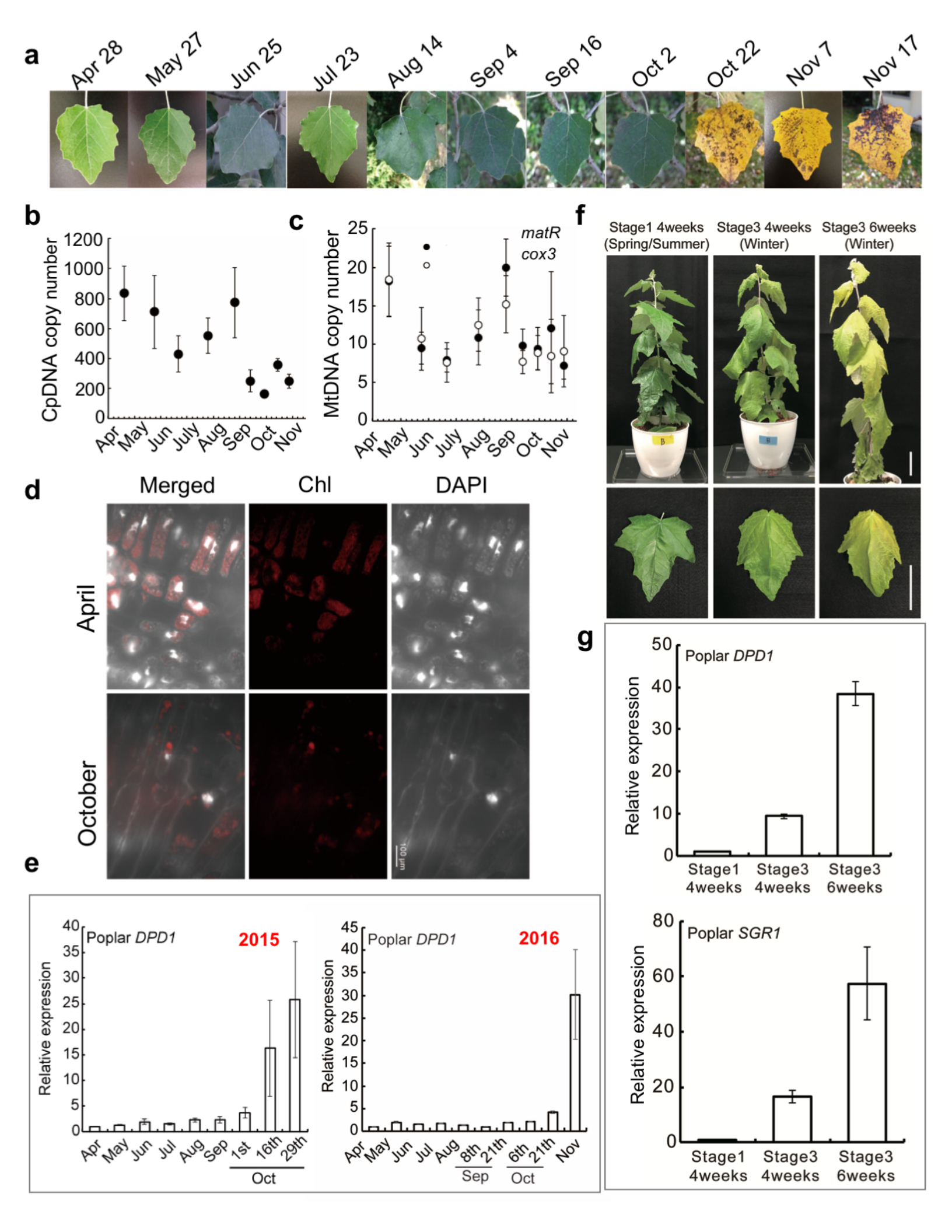
a
Apr 28
May 27
Jun 25
Jul 23
Aug 14
Sep 4
Sep 16
Oct 2
Oct 22
Nov 7
Nov 17
b
CpDNA copy number
1200
1000
800
600
400
200
0
Apr
May
Jun
July
Aug
Sep
Oct
Nov
c
MtDNA copy number
matR
cox3
25
20
15
10
5
0
Apr
May
Jun
July
Aug
Sep
Oct
Nov
f
Stage1 4weeks (Spring/Summer)
Stage3 4weeks (Winter)
Stage3 6weeks (Winter)
d
Merged
Chl
DAPI
April
October
100 μm
g
Poplar DPD1
Relative expression
50
40
30
20
10
0
Stage1 4weeks
Stage3 4weeks
Stage3 6weeks
Poplar SGR1
Relative expression
80
60
40
20
0
Stage1 4weeks
Stage3 4weeks
Stage3 6weeks
e
Poplar DPD1
2015
Relative expression
40
35
30
25
20
15
10
5
0
Apr
May
Jun
Jul
Aug
Sep
1st
16th
29th
Oct
Poplar DPD1
2016
Relative expression
45
40
35
30
25
20
15
10
5
0
Apr
May
Jun
Jul
Aug
8th
21th
Sep
6th
21th
Oct
Nov